 CMES, vol.28, no.3, pp.203-216, 2008

An Analysis for the Elasto-Plastic Fracture Problem by the Meshless Local Petrov-Galerkin Method

S.Y. Long[1,2,3], K.Y. Liu[1,2,4] and G.Y. Li[1]

Abstract: A meshless local Petrov-Galerkin method (MLPG) for the analysis of the elasto-plastic fracture problem is presented in this paper. The meshless method uses the moving least squares (MLS) to approximate the field functions. The shape function has not Kronecker Delta properties for the trial-function interpolation, and a direct interpolation method is adopted to impose essential boundary conditions. The MLPG method does not involve any domain and singular integrals if body force is ignored. It only involves a regular boundary integral. Two numerical examples show that results obtained by the present method have a good agreement with that by FEM software-ANSYS. However, in the present method, the computational time is greatly reduced in forming the tangent stiffness matrix because there is no domain integral, and the pre- and post-processing time are also greatly reduced because no element connectivity and no remeshing are required. The proposed method is valid and feasible for the solution of the elasto-plastic fracture problem.

Keyword: Meshless local Petrov-Galerkin method; Moving least squares; Heaviside function; direct interpolation method; Elasto-plastic fracture problem

1 Introduction

Atluri and Zhu originally proposed a meshless Petrov-Galerkin method(MLPG) [Atluri and Zhu (1998)], which is one of meshless methods. The MLPG method has many advantages over traditional numerical methods such as FEM and BEM. It has attracted much attention in the past decade due to its flexibility, and absolutely no elements or cells are needed in the formulation, either for interpolation purposes or for integration purposes. It requires only nodal information and no element connectivity is needed, which leads to a simple and convenient preprocessing. It is a truly meshless method. Remarkable successes of the MLPG method have been reported in solving convection–diffusion problems [Lin and Atluri (2000)]; fracture mechanics problems [Ching and Batra (2001)]; stress and crack analyses in 3-D axisymmetric FGM bodies [Sladek et al.(2005)]; dynamic fracture problems [Gao et al.(2006)]; fracture analyses in continuously nonhomogeneous piezoelectric solids [Sladek et al.(2007a)]; plate bending problems [Long and Atluri (2002); Gu and Liu (2001)]; analyses of shell deformations [Sladek et al.(2006a); Jarak et al.(2007)];heat conduction problems [Sladek et al.(2004); Wu et al.(2007)]; thermoelastic analyses [Ching and Chen (2006);Sladek et al.(2006b)]; thermo-piezoelectricity problems [Sladek et al.(2007b)]; magnetic diffution problems [Johnson and Owen (2007)]; wave problems [Ma (2005); Ma (2007)]; impact problems [Han et al.(2006); Liu et al.(2006)]; large deformation problems [Han et al.(2005)]; dynamics problems [Han and Atluri(2004); Andreaus et al.(2005)]; multiscale simulation problems [Bardenhagen and Kober (2004)]. Atluri and Shen presented six MLPG methods [Atluri and Shen (2002)] based on different test functions. One of methods named MLPG5 uses the Heaviside function as the test function. The applications of MLPG5 can be found in the works [Hu and Long

[1] State Key Laboratory of Advanced Design and Manufacture for Vehicle Body, Hunan University, Changsha, China
[2] College of Mechanics and Aerospace Engineering, Hunan University, Changsha, China
[3] Corresponding author. Tel.: +86-0731-8822114. E-mail: sylong@hnu.cn
[4] Mid-south Design & Research Institute, Changsha ,China

et al(2006); Long and Liu et al(2006); Liu and Long et al(2006)].

In this paper, the moving least squares(MLS) approximation scheme is used for constructing trial functions [Lancaster and Salkauskas (1981)], and a direct interpolation method [Liu and Yan (2000)] is used to impose the essential boundary condition since the MLS approximation does not satisfy the Kronecker delta function property. This simple and effective treatment is made possible because the MLPG method establishes discrete equations node by node. In this paper MLPG5 method is used to solve the elasto-plastic fracture problem.

2 Elasto-plastic stress-strain relation for plane problems [Crisfield (1991); Owen and Hinton (1980); Wang and Shao (1997)]

The basic laws governing elasto-plastic material behavior in a two dimensional solid must be presented before the numerical aspects of a problem can be considered. Only the essential expressions will be provided in this section and reader will be directed to other sources for a more complete theoretical treatment.

The object of the plasticity theory is to provide a theoretical description of the relationship between stress and strain for a material which exhibits an elasto-plastic response. In essence, plastic behavior is characterized by an irreversible straining which is time dependent and which can only be sustained once a certain level of stress has been reached. In this section we outline the elasto-plastic stress-strain relation for the plane problems.

For plane problems, we have only four non-zero stress components, namely in the vector form

$$\boldsymbol{\sigma}^T = \begin{cases} \begin{bmatrix} \sigma_x & \sigma_y & \tau_{xy} \end{bmatrix}, & \sigma_z = 0 \\ & \text{for plane stress} \\ \begin{bmatrix} \sigma_x & \sigma_y & \sigma_z & \tau_{xy} \end{bmatrix}, & \varepsilon_z = 0 \\ & \text{for plane strain} \end{cases} \tag{1}$$

For the plane stress problem, for example, the incremental stress and strain components can be written as, respectively, in the matrix form

$$\mathrm{d}\boldsymbol{\sigma}^T = \begin{bmatrix} \mathrm{d}\sigma_x & \mathrm{d}\sigma_y & \mathrm{d}\tau_{xy} \end{bmatrix} \tag{2}$$

$$\mathrm{d}\boldsymbol{\varepsilon}^T = \begin{bmatrix} \mathrm{d}\varepsilon_x & \mathrm{d}\varepsilon_y & \mathrm{d}\gamma_{xy} \end{bmatrix} \tag{3}$$

The complete elasto-plastic incremental stress-strain relation can be written as

$$\mathrm{d}\boldsymbol{\sigma} = \mathbf{D}^{ep}\mathrm{d}\boldsymbol{\varepsilon} \tag{4}$$

Where

$$\mathbf{D}^{ep} = \mathbf{D}^e - \mathbf{D}^p \tag{5}$$

in which $\mathbf{D}^p$ is termed the matrix of plastic material behavior.

The explicit form of the elastic matrix $\mathbf{D}^e$ for the plane stress problem can be written as

$$\mathbf{D}^e = \frac{E}{1-\nu}\begin{bmatrix} 1 & \nu & 0 \\ \nu & 1 & 0 \\ 0 & 0 & 1-\nu/2 \end{bmatrix} \tag{6}$$

in which E and ν are respectively the elastic modulus and Poisson's ratio of the material.

The yield criterion for the isotropic hardening material can be expressed as

$$F = f - k = 0 \tag{7}$$

where for the plane stress problem

$$f = \frac{1}{2}\left(S_x^2 + S_y^2 + S_z^2 + 2\tau_{xy}^2\right), \quad k = \frac{1}{3}\overline{\sigma}^2 \tag{8}$$

and

$$S_x = \sigma_x - \frac{1}{3}(\sigma_x + \sigma_y) = \frac{1}{3}(2\sigma_x - \sigma_y) \tag{9a}$$

$$S_y = \sigma_y - \frac{1}{3}(\sigma_x + \sigma_y) = \frac{1}{3}(2\sigma_y - \sigma_x) \tag{9b}$$

$$S_z = -\frac{1}{3}(\sigma_x + \sigma_y) \tag{9c}$$

Stress states for $f = k$ represent plastic states, while elastic behavior is characterized by $f < k$. At a plastic state, $f = k$, the incremental change in the yield function due to an incremental stress change is

$$\mathrm{d}f = \frac{\partial f}{\partial \boldsymbol{\sigma}}\mathrm{d}\boldsymbol{\sigma} \tag{10}$$

Then if

$df > 0$ plastic loading (plastic behavior for a strain hardening material) and the stress point remains on the expanding yield surface.

$df < 0$ elastic unloading occurs (elastic behavior) and the stress point returns inside the yield surface.

$df = 0$ neutral loading (plastic behavior for a perfectly plastic material) and the stress point remains on the yield surface.

The above is just loading or unloading criterion by which we can select the elasto-plastic constitutive equation or the elasto constitutive equation in computation.

For the isotropic hardening and perfectly plastic material, we have

$$\frac{\partial f}{\partial \boldsymbol{\sigma}} = \begin{bmatrix} S_x & S_y & 2\tau_{xy} \end{bmatrix}^T \tag{11}$$

Thus we obtain the matrix of plastic material behavior $\mathbf{D}^p$

$$\mathbf{D}^p = \frac{E}{B(1-\nu^2)} \begin{bmatrix} (S_x+\nu S_y)^2 & (S_x+\nu S_y)(S_y+\nu S_x) & (1-\nu)(S_x+\nu S_y)\tau_{xy} \\ & (S_y+\nu S_x)^2 & (1-\nu)(S_y+\nu S_x)\tau_{xy} \\ Sym & & (1-\nu)^2\tau_{xy}^2 \end{bmatrix} \tag{12}$$

in which

$$B = S_x^2 + S_y^2 + 2\nu S_x S_y + 2(1-\nu)\tau_{xy}^2 + \frac{2(1-\nu)H'\overline{\sigma}^2}{9\nu} \tag{13}$$

Where $\overline{\sigma}$ is termed the effective stress or equivalent stress,which can be expressed as for the plane stress problem

$$\overline{\sigma} = (\sigma_1^2 + \sigma_2^2 - \sigma_1\sigma_2)^{\frac{1}{2}} \tag{14}$$

where σ_1, σ_2 are the principle sresses. H' in equation(12) is called a plastic modulus or hardening function, which can be determined experimentally from a simple uniaxial yield test.

By substituting equations (6) and (12) into equation (5), the matrix form of elasto-plastic material behavior can be expressed as

$$\mathbf{D}^{ep} = \frac{E}{B} \begin{bmatrix} S_y^2+2P & -S_xS_y+2\nu P & -\frac{S_x+\nu S_y}{1+\nu}\tau_{xy} \\ & S_x^2+2P & -\frac{S_y+\nu S_x}{1+\nu}\tau_{xy} \\ Sym & & \frac{R}{2(1+\nu)} + \frac{2(1-\nu)H'\overline{\sigma}^2}{9\nu} \end{bmatrix} \tag{15}$$

where

$$P = \frac{2H'\overline{\sigma}^2}{9E} + \frac{\tau_{xy}^2}{1+\nu} \tag{16}$$

$$R = S_x^2 + 2\nu S_x S_y + S_y^2 \tag{17}$$

$$B = R + 2(1-\nu^2)P \tag{18}$$

For the plane strain problem after yielding of a material the Poisson's ratio is taken as 0.5. Here on substituting this value into equation (15) and replacing E and ν by $\frac{E}{1-\nu^2}$ and $\frac{\nu}{1-\nu}$ respectively the elasto-plastic matrix $\mathbf{D}^{ep}$ can be directly obtained.

3 The MLPG formulation of the incremental analysis for elasto-plastic problems

An incremental solution scheme in which an applied load is divided into a series of incremental ones, must be employed in the elasto-plastic analysis of a structure, since the elasto-plastic behaviors of the structure are related to the loading and deformation history. Within each incremental load the elasto-plastic equations solved are linearized, then the solution for a nonlinear problem is decomposed into a series of solutions for linear problems.

Assume that displacements ${}^t u_i$, strain ${}^t \varepsilon_{ij}$ and stress ${}^t \sigma_{ij}$ at time t are found under the prescribed load or displacement, then at time $t+\Delta t$, both applied loads including body forces and tractions, and prescribed displacements should have increments and be known, i.e.

$${}^{t+\Delta t} b_i = {}^t b_i + \Delta b_i \quad \text{in } \Omega \tag{19}$$

$${}^{t+\Delta t} \overline{T}_i = {}^t \overline{T}_i + \Delta \overline{T}_i \quad \text{on } \Gamma_t \tag{20}$$

$${}^{t+\Delta t} \overline{u}_i = {}^t \overline{u}_i + \Delta \overline{u}_i \quad \text{on } \Gamma_u \tag{21}$$

where b_i, T_i and u_i denote components of body forces, tractions and displacements, respectively. Now we will find displacements, strains and stresses at time $t+\Delta t$

$$\left.\begin{array}{l} {}^{t+\Delta t}u_i = {}^{t}u_i + \Delta u_i \\ {}^{t+\Delta t}\varepsilon_{ij} = {}^{t}\varepsilon_{ij} + \Delta\varepsilon_{ij} \\ {}^{t+\Delta t}\sigma_{ij} = {}^{t}\sigma_{ij} + \Delta\sigma_{ij} \end{array}\right\} \tag{22}$$

which must satisfy the following equations and boundary conditions:
equilibrium equation

$${}^{t}\sigma_{ij,j} + \Delta^{t}\sigma_{ij,j} + {}^{t}b_i + \Delta b_i = 0 \quad \text{in } \Omega \tag{23}$$

geometrical equation

$${}^{t}\varepsilon_{ij} + \Delta^{t}\varepsilon_{ij} = \frac{1}{2}\left({}^{t}u_{ij} + {}^{t}u_{ji}\right)\frac{1}{2}\left(\Delta^{t}u_{ij} + \Delta^{t}u_{ji}\right) \tag{24}$$

stress-strain relation or constitutive equation

$$\Delta\sigma_{ij} = {}^{\tau}D^{ep}_{ijkl}\Delta\varepsilon_{kl} \quad t \le \tau \le t+\Delta t \tag{25}$$

boundary conditions

$${}^{t}T_i + \Delta T_i = {}^{t}\overline{T}_i + \Delta\overline{T}_i \quad \text{on } \Gamma_t \tag{26}$$

$${}^{t}u_i + \Delta u_i = {}^{t}\overline{u}_i + \Delta\overline{u}_i \quad \text{on } \Gamma_u \tag{27}$$

where

$${}^{t}T_i = {}^{t}\sigma_{ij}n_j, \quad \Delta T_i = \Delta\sigma_{ij}n_j \tag{28}$$

where n_j is a unit outward normal to the boundary Γ.

It should be noted that except the stress-strain relation other equations and boundary conditions are linear for the elasto-plastic analysis under the small deformation.

In a similar way to creating the MLPG formulation for the linear elastic problem [Hu and Long(2006)], we use two different sets of equations for the essential boundary nodes and not essential boundary nodes, respectively.

For node not located on the essential boundary, we start from a weak form over a local sub-domain Ω_s and use the MLS approximation to develop the present MLPG formulation for the elasto-plastic problem in which the local sub-domain Ω_s is set to βd_i^1, β is a scaling factor for determining the sub-domain and d_i^1 is the distance to the nearest neighboring point from node i. Here we set $\beta \le 1.0$ to make the sub-domain Ω_s not intersect with the essential boundary Γ_u, so a generalized local weak form of Eq.(23) over a sub-domain Ω_s can be written as follows

$$\int_{\Omega_s} v_i\left({}^{t}\sigma_{ij,j} + \Delta\sigma_{ij,j} + {}^{t}b_i + \Delta b_i\right)d\Omega = 0 \tag{29}$$

where v_i is the test functions. Using the relationship

$$\Delta\sigma_{ij,j}v_i = \left(\Delta\sigma_{ij}v_i\right)_{,j} - \Delta\sigma_{ij}v_{i,j} \tag{30}$$

and

$${}^{t}\sigma_{ij,j}v_i = \left({}^{t}\sigma_{ij}v_i\right)_{,j} - {}^{t}\sigma_{ij}v_{i,j} \tag{31}$$

and the divergence theorem as well as Eq.(28) in Eq.(29) leads to

$$\int_{\partial\Omega_s}({}^{t}T_i + \Delta T_i)v_i d\Gamma + \int_{\Omega_s}(-{}^{t}\sigma_{ij}v_{i,j} - \Delta\sigma_{ij}v_{i,j} + {}^{t}b_i v_i + \Delta b_i v_i)\mathrm{d}\Omega = 0 \tag{32}$$

where $\partial\Omega_s$ is the boundary of the sub-domain Ω_s. In general, $\partial\Omega_s = \Gamma_s \cup L_s$ with Γ_s being the part of the local boundary located on the global boundary Γ and L_s being the other part of the local boundary over which no boundary condition is specified, i.e. $\Gamma_s = \partial\Omega_s \cap \Gamma$ and $\Gamma_s = \partial\Omega_s - L_s$.

It should be mentioned that Eq.(32) holds regardless of the size and the shape of Ω_s provided that Ω_s is smooth enough for the divergence theorem to apply. So, the shape of sub-domain Ω_s can be taken to be a circle in the two dimensional problem without loosing generality.

Applying the natural boundary condition, ${}^{t}T_i = {}^{t}\sigma_{ij}n_j = {}^{t}\overline{T}_i$ and $\Delta T_i = \Delta\sigma_{ij}n_j = \Delta\overline{T}_i$ on Γ_{st} where $\Gamma_{st} = \partial\Omega_s \cap \Gamma_t$, we get

$$\int_{L_s}({}^{t}T_i + \Delta T_i)v_i d\Gamma + \int_{\Gamma_{st}}({}^{t}\overline{T}_i + \Delta\overline{T}_i)v_i d\Gamma - \int_{\Omega_s}({}^{t}\sigma_{ij} + \Delta\sigma_{ij})v_{i,j}d\Omega + \int_{\Omega_s}({}^{t}b_i + \Delta b_i)v_i\mathrm{d}\Omega = 0 \tag{33}$$

In order to simplify Eq.(33), test functions v_i are chosen such that they simplify the domain integral on Ω_s. This can be accomplished by using the Heaviside step function

$$H(x)=\begin{cases} c & x\in\Omega_s \\ 0 & x\notin\Omega_s \end{cases} \tag{34}$$

where c is an arbitrary constant($c=1$ is used in this study). Using the choice, the partial derivatives of the test function $v_{i,j}$ are identically zero, hence the corresponding domain integrals involved in Eq.(33) are identically zero. Using this test function and rearranging Eq.(33), we obtain the following local symmetric weak form

$$\begin{aligned}\int_{L_s}\Delta T_i d\Gamma =& \\ -\int_{\Gamma_{st}}\left({}^t\overline{T}_i+\Delta\overline{T}_i\right)d\Gamma-&\int_{\Omega_s}\left({}^t b_i+\Delta b_i\right)\mathrm{d}\Omega \\ &-\int_{L_s}{}^t T_i d\Gamma\end{aligned} \tag{35}$$

For simplicity, Eq.(35) can be written in the matrix form as

$$\begin{aligned}\int_{L_s}\Delta\mathbf{T}d\Gamma=-\int_{\Gamma_{st}}&\left({}^t\overline{\mathbf{T}}+\Delta\overline{\mathbf{T}}\right)d\Gamma \\ &-\int_{\Omega_s}({}^t\mathbf{b}+\Delta\mathbf{b})\mathrm{d}\Omega-\int_{L_s}{}^t\mathbf{T}d\Gamma\end{aligned} \tag{36}$$

where

$$\begin{aligned}{}^t\overline{\mathbf{T}}&=\begin{Bmatrix}{}^tT_1\\ {}^tT_2\end{Bmatrix},\quad \Delta\mathbf{T}=\begin{Bmatrix}\Delta T_1\\ \Delta T_2\end{Bmatrix}, \\ {}^t\mathbf{b}&=\begin{Bmatrix}{}^tb_1\\ {}^tb_2\end{Bmatrix},\quad \Delta\mathbf{b}=\begin{Bmatrix}\Delta b_1\\ \Delta b_2\end{Bmatrix}\end{aligned} \tag{37}$$

In order to obtain the discretized system equation, the global problem domain Ω is represented by properly distributed field nodes and using the MLS shape function to approximate the trial function for the incremental displacement at a point x

$$\begin{aligned}\Delta\mathbf{u}^h(x)&=\begin{Bmatrix}\Delta u^h\\ \Delta v^h\end{Bmatrix} \\ &=\begin{bmatrix}\varphi_1 & 0 & \cdots & \varphi_n & 0\\ 0 & \varphi_1 & \cdots & 0 & \varphi_n\end{bmatrix}\begin{Bmatrix}\Delta\widehat{u}_1\\ \Delta\widehat{v}_1\\ \vdots\\ \Delta\widehat{u}_n\\ \Delta\widehat{v}_n\end{Bmatrix} \\ &=\mathbf{\Phi}\Delta\widehat{\mathbf{u}}\end{aligned} \tag{38}$$

where n is the number of nodes in the support domain of a sampling point at x, and $\mathbf{\Phi}$ is the matrix of the MLS shape functions, $\Delta\widehat{\mathbf{u}}$ is the fictitious nodal value of $\Delta\mathbf{u}$.

Substituting the MLS approximation (38) into Eq.(36) leads to the following nodal discretized equation of the MLPG for the I th field node.

$$\begin{aligned}\int_{L_s}\mathbf{n}^\tau\mathbf{D}^{ep}\mathbf{B}\Delta\hat{\mathbf{u}}\mathrm{d}\Gamma=&-\int_{\Gamma_{st}}{}^{t+\Delta t}\overline{\mathbf{T}}\mathrm{d}\Gamma \\ &-\int_{\Omega_s}{}^{t+\Delta t}\mathbf{b}\mathrm{d}\Omega-\int_{L_s}\mathbf{n}^t\boldsymbol{\sigma}\mathrm{d}\Gamma\end{aligned} \tag{39}$$

where $\mathbf{n}$ is a matrix of the unit outward normal to the local boundary L_s. It is given by

$$\mathbf{n}=\begin{bmatrix}n_1 & 0 & n_2\\ 0 & n_2 & n_1\end{bmatrix} \tag{40}$$

Using the strain-displacement equation for small deformation, we can have

$$\mathbf{B}=\begin{bmatrix}\frac{\partial\varphi_1}{\partial x_1} & 0 & \cdots & \frac{\partial\varphi_n}{\partial x_1} & 0\\ 0 & \frac{\partial\varphi_1}{\partial x_2} & \cdots & 0 & \frac{\partial\varphi_n}{\partial x_2}\\ \frac{\partial\varphi_1}{\partial x_2} & \frac{\partial\varphi_1}{\partial x_1} & \cdots & \frac{\partial\varphi_n}{\partial x_2} & \frac{\partial\varphi_n}{\partial x_1}\end{bmatrix} \tag{41}$$

Summing over all nodes that not located on the essential boundary leads the following discretized system equation

$$\begin{aligned}{}^\tau\mathbf{K}_{Ij}^{ep}\Delta\hat{\mathbf{u}}_j&=\Delta\mathbf{Q}_I \\ &(I=1,2,...,N-k,\quad j=1,2,...,N)\end{aligned} \tag{42}$$

where N is the total number of field nodes, and k is the number of nodes located on the essential boundary, where

$${}^\tau\mathbf{K}_{ij}^{ep}=\int_{L_s}\mathbf{n}^\tau\mathbf{D}^{ep}\mathbf{B}_j\mathrm{d}\Gamma \tag{43}$$

$${}^{t+\Delta t}\mathbf{Q}_e=-\int_{\Gamma_{st}}{}^{t+\Delta t}\overline{\mathbf{T}}\mathrm{d}\Gamma-\int_{\Omega_s}{}^{t+\Delta t}\mathbf{b}\mathrm{d}\Omega \tag{44}$$

$${}^t\mathbf{Q}_i=\int_{L_s}\mathbf{n}^t\boldsymbol{\sigma}\mathrm{d}\Gamma \tag{45}$$

in which ${}^{t+\Delta t}\mathbf{Q}_e$ and ${}^t\mathbf{Q}_i$ denote the external load vector and internal load vector respectively, and $\Delta\mathbf{Q}_I$ is called as a non-equilibrium force vector. When ${}^{t+\Delta t}\mathbf{Q}_e$ and ${}^t\mathbf{Q}_i$ satisfy the equilibrium equation, then $\Delta\mathbf{Q}_I$ represents the incremental load vector. It should be noted j is the number

of nodes within the support domain of a field point x and is not determined.

For node j located on the essential boundary, a direct interpolation method for the imposition of essential boundary conditions is introduced. This method was proposed by Liu and Yan(2000) to simplify the MLPG formulation. The direct interpolation method enforces the essential boundary conditions using the equation of the MLS approximation

$$\begin{aligned}\Delta\mathbf{u}_j^h &= \begin{Bmatrix}\Delta u^h \\ \Delta v^h\end{Bmatrix}_j \\ &= \begin{bmatrix}\varphi_1 & 0 & \cdots & \varphi_n & 0 \\ 0 & \varphi_1 & \cdots & 0 & \varphi_n\end{bmatrix} \begin{Bmatrix}\Delta\widehat{u}_1 \\ \Delta\widehat{v}_1 \\ \vdots \\ \Delta\widehat{u}_n \\ \Delta\widehat{v}_n\end{Bmatrix} \\ &= \begin{Bmatrix}\Delta\overline{u} \\ \Delta\overline{v}\end{Bmatrix}_j\end{aligned} \tag{46}$$

where $\Delta\overline{u}_j$ and $\Delta\overline{v}_j$ are the specified displacement at node j on the essential boundary. Eq.(46) is still a linear algebraic equation for node j on the essential boundary in the elasto-plastic analysis under small deformation, and is directly assembled into the global system equation. This treatment of the essential boundary condition is straight forward and very effective. It simplify significantly the procedure of imposing essential boundary conditions and the essential boundary conditions are satisfied exactly. Moreover, computation for all the nodes on the essential boundary has been simplified. This simple treatment is made possible become the MLPG method establishes discrete equations node by node.

Integrating Eq.(46) into Eq.(42), the global discretized system equation is finally obtained as

$$^{\tau}\mathbf{K}^{ep}\Delta\hat{\mathbf{u}} = \Delta\mathbf{Q} \tag{47}$$

where forms of $^{\tau}\mathbf{K}^{ep}$ and $\Delta\mathbf{Q}$ are similar to that of the stiffness matrix $\mathbf{K}$ and the load vector $\mathbf{f}$ for the linear elastic problem, reader may refer to Chapter 5 of Reference [Liu and Gu (2005)].

4 Basic numerical solution processes [Crisfield (1991); Owen and Hinton (1980); Wang and Shao (1997)]

4.1 The Newton-Raphson iteration and increment procedure

A combined incremental and iterative solution procedure using the Newton- Raphson iteration is commonly employed to solve the system of nonlinear equation (47). Thus equation (47) can be rewritten as

$$^{t+\Delta t}\mathbf{K}^{ep(n)}\Delta\hat{\mathbf{u}}^{(n)} = \Delta\mathbf{Q}^{(n)} \tag{48}$$

in which n is the iterative number ($n = 1, 2, \ldots$) and

$$\left.\begin{aligned}^{t+\Delta t}\mathbf{K}^{ep(n)} &= \textstyle\int_{L_s}\mathbf{n}^{t+\Delta t}\mathbf{D}^{ep(n)}\mathbf{B}\mathrm{d}\Gamma \\ \Delta\mathbf{Q}^{(n)} &= {}^{t+\Delta t}\mathbf{Q}_e - \textstyle\int_{L_s}\mathbf{n}^{t+\Delta t}\boldsymbol{\sigma}^{(n)}\mathrm{d}\Gamma\end{aligned}\right\} \tag{49}$$

in which

$$\left.\begin{aligned}^{t+\Delta t}\mathbf{D}^{ep} &= \mathbf{D}^{ep}\left({}^{t+\Delta t}\boldsymbol{\sigma}^{(n)}, {}^{t+\Delta t}\overline{\varepsilon}^{p(n)}\right) \\ {}^{t+\Delta t}\boldsymbol{\sigma}^{(0)} &= {}^{t}\boldsymbol{\sigma}, {}^{t+\Delta t}\overline{\varepsilon}^{p(0)} = {}^{t}\overline{\varepsilon}^{p}\end{aligned}\right\} \tag{50}$$

It should be noted that Eq.(48) is just equal to Eq.(47) in time $\tau = t$ when $n = 0$.

Using Eq.(48) the procedures for computing fictitious incremental nodal displacements, $\Delta\hat{\mathbf{u}}^{(n)}$, is as follow:

a) Compute $^{t+\Delta t}\mathbf{K}^{ep(n)}$, $\Delta\mathbf{Q}^{(n)}$ from Eq.(49);

b) Solve Eq.(48) to obtain fictitious incremental nodal displacements in the current iterative step

$$\Delta\hat{\mathbf{u}}^{(n)} = \left({}^{t+\Delta t}\mathbf{K}^{ep(n)}\right)^{-1}\Delta\mathbf{Q}^{(n)} \tag{51}$$

c) Find incremental nodal displacements $\Delta\mathbf{u}^{(n)}$ and the total displacements $^{t+\Delta t}\mathbf{u}^{(n+1)}$ at any point x of a problem domain considered using Eq.(38), i.e.

$$\begin{aligned}\Delta\mathbf{u}^{(n)} &= \boldsymbol{\Phi}\Delta\widehat{\mathbf{u}}^{(n)} \\ {}^{t+\Delta t}\mathbf{u}^{(n+1)} &= {}^{t+\Delta t}\mathbf{u}^{(n)} + \Delta\mathbf{u}^{(n)}\end{aligned} \tag{52}$$

d) Compute incremental strains and incremental stresses from the following equations

$$\Delta\boldsymbol{\varepsilon}^{(n)} = \mathbf{B}\Delta\mathbf{u}^{(n)} \tag{53}$$

$$\Delta\boldsymbol{\sigma}^{(n)} = \int_0^{\Delta\varepsilon^{p(n)}} \mathbf{D}^{ep}\mathrm{d}\varepsilon \tag{54}$$

in which $\Delta\boldsymbol{\varepsilon}^{p(n)}$ is the part of plastic incremental strains of $\Delta\boldsymbol{\varepsilon}^{(n)}$, and integration of Eq.(54) and computation of $\Delta\boldsymbol{\varepsilon}^{p(n)}$ will be discussed in the following. The total stresses in time $t+\Delta t$, ${}^{t+\Delta t}\boldsymbol{\sigma}^{(n+1)}$, can be obtained

$${}^{t+\Delta t}\boldsymbol{\sigma}^{(n+1)} = {}^{t+\Delta t}\boldsymbol{\sigma}^{(n)} + \Delta\boldsymbol{\sigma}^{(n)} \tag{55}$$

e) Check convergence using one of the following convergence criteria:
displacement convergence criterion:

$$\left\|\Delta\mathbf{u}^{(n)}\right\| \le er_D \left\|{}^{t}\mathbf{u}\right\| \tag{56}$$

equilibrium convergence criterion:

$$\left\|\Delta\mathbf{Q}^{(n)}\right\| \le er_F \left\|\Delta\mathbf{Q}^{(0)}\right\| \tag{57}$$

in which er_D and er_F are the prescribed tolerances.

If the convergence criterion is already satisfied, the iteration within the current load incremental step is considered to be convergent. For each load incremental step the above a)∼e) procedures are performed until the solution in the total time is obtained.

4.2 Determination of the elasto-plastic states

We well know from the above discuss that determination of ${}^{\tau}\mathbf{D}^{ep}$ and $\Delta\mathbf{Q}^{(n)}$ in Eq.(47) is dependent on ${}^{t}\boldsymbol{\sigma}$ and ${}^{t}\overline{\varepsilon}^{p}$ obtained in the previous load increment step or at the end of the iteration process. For the next load increment or iteration step $\Delta\boldsymbol{\sigma}$, $\Delta\overline{\varepsilon}^{p}$ and other related quantities can be obtained from incremental displacements in the current load increment or iteration step, thus $\boldsymbol{\sigma}$, $\overline{\varepsilon}^{p}$ and other related quantities can also be obtained, i.e. the elasto-plastic state in the current load increment or iteration step is perfectly determined.

After obtaining the incremental displacements of each load increment or iteration step, the basic algorithm for determination of a new elasto-plastic state is as follows:

1. Compute incremental strains (or iterative modified strains) $\Delta\boldsymbol{\varepsilon}$ using geometric equations.

2. Compute predictors of incremental stresses and stresses using elastic constitutive equations, i.e.

$$\Delta\tilde{\boldsymbol{\sigma}} = \mathbf{D}^{e}\Delta\boldsymbol{\varepsilon} \tag{58}$$

$${}^{t+\Delta t}\tilde{\boldsymbol{\sigma}} = {}^{t}\boldsymbol{\sigma} + \Delta\tilde{\boldsymbol{\sigma}} \tag{59}$$

in which ${}^{t}\boldsymbol{\sigma}$ is the stress value at the end of the previous incremental step.

3. Compute predictors of matrix $\mathbf{D}$ for each Gaussian point in each sub-domain

4. Compute the value of the yield function $F\left({}^{t+\Delta t}\tilde{\boldsymbol{\sigma}},\, {}^{t}\overline{\varepsilon}^{p}\right)$. In terms of this value three cases are divided:

   i. When $F\left({}^{t+\Delta t}\tilde{\boldsymbol{\sigma}},\, {}^{t}\overline{\varepsilon}^{p}\right) \le 0$, elastic loading or elastic unloading from the yield surface occurs at this integral point, i.e.

   $$\Delta\boldsymbol{\sigma} = \Delta\tilde{\boldsymbol{\sigma}} \tag{60}$$

   ii. When $F\left({}^{t+\Delta t}\tilde{\boldsymbol{\sigma}},\, {}^{t}\overline{\varepsilon}^{p}\right) > 0$ and $F\left({}^{t}\boldsymbol{\sigma},\, {}^{t}\overline{\varepsilon}^{p}\right) < 0$, a transition state between elasticity and plasticity arrives at this integral point. A scaling factor m, which determines arrival time of stresses at the yield surface, is computed using the following expression

   $$F\left({}^{t}\boldsymbol{\sigma} + m\Delta\tilde{\boldsymbol{\sigma}},\, {}^{t}\overline{\varepsilon}^{p}\right) = 0 \tag{61}$$

   iii. When $F\left({}^{t+\Delta t}\tilde{\boldsymbol{\sigma}},\, {}^{t}\overline{\varepsilon}^{p}\right) > 0$ and $F\left({}^{t}\boldsymbol{\sigma},\, {}^{t}\overline{\varepsilon}^{p}\right) = 0$, plastic loading at this integral point remains and here $m = 0$.

5. Compute the part of plastic incremental strains of $\Delta\boldsymbol{\varepsilon}$

$$\Delta\boldsymbol{\varepsilon}^{p} = (1-m)\Delta\boldsymbol{\varepsilon} \tag{62}$$

6. Compute the corresponding plastic incremental stresses

$$\Delta\sigma^{p} = \int_0^{\Delta\varepsilon^{p}} \mathbf{D}^{ep}(\boldsymbol{\sigma}, \overline{\varepsilon}^{p})\mathrm{d}\varepsilon \tag{63}$$

7. Compute ${}^{t+\Delta t}\boldsymbol{\sigma}$ and ${}^{t+\Delta t}\overline{\varepsilon}^p$ at the current load increment step or at the end of the iteration process

$${}^{t+\Delta t}\boldsymbol{\sigma} = {}^{t}\boldsymbol{\sigma} + m\Delta\boldsymbol{\sigma} + \Delta\boldsymbol{\sigma}^p \tag{64}$$

$${}^{t+\Delta t}\overline{\varepsilon}^p = {}^{t}\overline{\varepsilon}^p + \Delta\overline{\varepsilon}^p \tag{65}$$

4.3 Integrating of the constitutive equation

A sub-increment with a tangential predictor and radial-return algorithm and a generalized mid-point algorithm are commonly employed for integrating of the constitutive equation (63). Here the former will be employed.

By the tangential predictor is meant in application of the Euler procedure to equation (62) the predictor of the incremental stress is obtained, i.e.

$$\Delta\tilde{\boldsymbol{\sigma}} = \mathbf{D}^{ep}\left({}^{t}\boldsymbol{\sigma}, {}^{t}\overline{\varepsilon}^p\right)\Delta\boldsymbol{\varepsilon} \tag{66}$$

Thus the stress predictor is further obtained

$${}^{t+\Delta t}\tilde{\boldsymbol{\sigma}} = {}^{t}\boldsymbol{\sigma} + \Delta\tilde{\boldsymbol{\sigma}} \tag{67}$$

Therefore we can obtain

$$\Delta\overline{\varepsilon}^p = \frac{2}{3}\Delta\lambda\,\overline{\sigma} \tag{68}$$

$${}^{t+\Delta t}\overline{\varepsilon}^p = {}^{t}\overline{\varepsilon}^p + \Delta\overline{\varepsilon}^p \tag{69}$$

where $\mathbf{D}^{ep}\left({}^{t}\boldsymbol{\sigma}, {}^{t}\overline{\varepsilon}^p\right)$ is an initial tangential stiffness matrix, hence the predictor of the incremental stress $\Delta\tilde{\boldsymbol{\sigma}}$ lies along the tangent to the yield surface. It is clear that the stress predictor ${}^{t+\Delta t}\tilde{\boldsymbol{\sigma}}$ lies outside the yield surface since the yield surface is convex. However, the yield criterion requires ${}^{t+\Delta t}\tilde{\boldsymbol{\sigma}}$ lies on or within the yield surface, the radial-return algorithm must be employed to return the stresses to the yield surface so that the yield criterion is satisfied.

We can assume

$${}^{t+\Delta t}\boldsymbol{\sigma} = r\,{}^{t+\Delta t}\tilde{\boldsymbol{\sigma}} \tag{70}$$

in which r is a scaling factor. Thus we can find scaling factor r from yield criterion

$$F\left({}^{t+\Delta t}\boldsymbol{\sigma}, {}^{t+\Delta t}\overline{\varepsilon}^p\right) = 0 \tag{71}$$

as

$$r = \left(\frac{2}{3}\overline{\boldsymbol{\sigma}}^2/\mathbf{S}^T\mathbf{S}\right)^{1/2}$$

It should be mentioned that even though corrected stresses ${}^{t+\Delta t}\boldsymbol{\sigma}$ through the radial-return algorithm lie on the yield surface, the tangential stiffness matrix may be inconsistent with the integration scheme since the incremental strain $\Delta\boldsymbol{\varepsilon}$ and effective plastic strain ${}^{t+\Delta t}\overline{\varepsilon}^p$ are assumed to be constant. The error can be significantly reduced by sub-increment. Using such a technique the incremental strains $\Delta\boldsymbol{\varepsilon}$ is divided into$m$ sub-steps each of $q\Delta\boldsymbol{\varepsilon}$, where $q = 1/m$ and the tangent procedure is applied at each sub-step. The elasto-plastic state at the end of each sub-step is considered as the initial state for the next sub-step. Finally we can obtain the consistent tangent stiffness matrix with the integration scheme, hence consistent ${}^{t+\Delta t}\boldsymbol{\sigma}$ and ${}^{t+\Delta t}\overline{\varepsilon}^p$.

5 Numerical examples

The MLPG method is applied to analyze the elasto-plastic fracture problems. In all following examples, the Von Mises yield criterion and isotropic linear hardening are used for the elasto-plastic materials. The field functions are constructed using the moving least square approximation, in which the quadratic basis function is adopted and the Gaussian function is chosen as the weighted function. For the numerical integration, 9 Gauss points are assigned on boundaries L_s and Γ_s for the boundary integral unless otherwise specified.

5.1 Example 1: a both edge-cracked square plate

A both edge-cracked square plate with both length and width $L = 200$mm, and crack length $a = 50$mm, subjected to the uniformly distributed tensile stress $\overline{t} = 500$MPa at both top and bottom edges of the plate, as shown in Fig.1, was discussed. Here we assume elastic modulus $E = 200$GPa, Poisson's ratio $\nu = 0.3$,the tangent elastic modulus $E^t = 50$GPa, the initial yield stress $\sigma_{s0} = 800$MPa. Due to symmetry of geometry

and load, a quadrant of the plate is analyzed and is assumed to be the plane stress problem. In computation, a meshless discretization consisting of 472 nodes is used, and symmetric displacement boundary conditions are imposed, as shown in Fig.2. The load increment is taken as $\Delta\bar{t} = 0.1 \times \bar{t}$, i.e. 10 load incremental steps are divided.

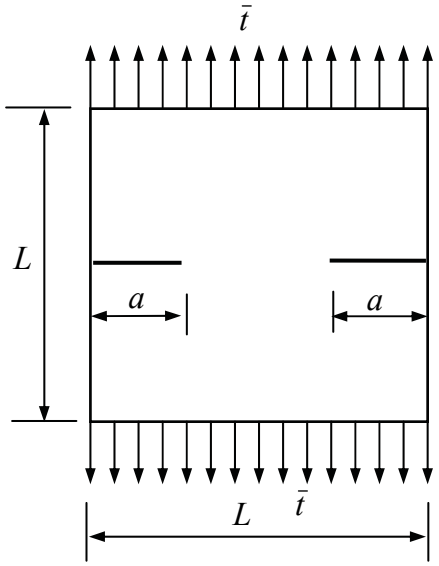

Figure 1: A both edge-cracked square plate

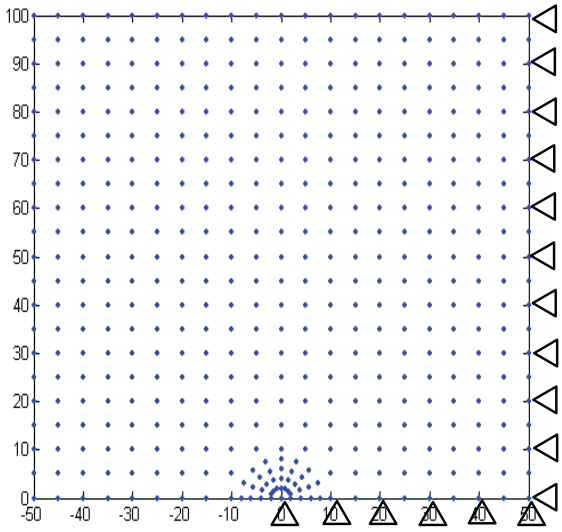

Figure 2: A meshless discretization (472nodes) and boundary conditions

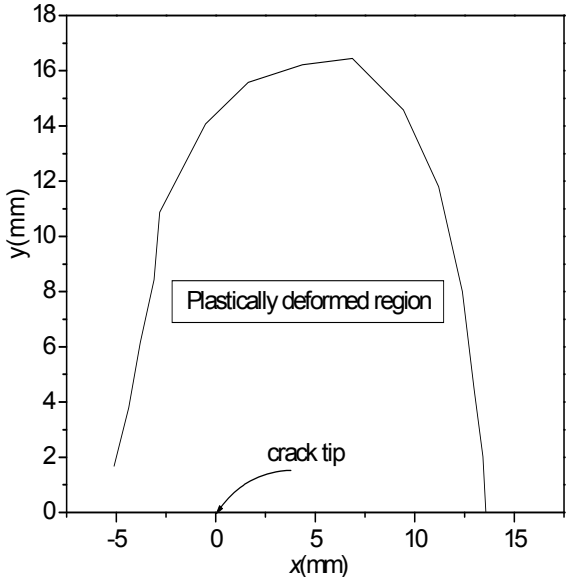

Figure 3: The plastically deformed region at the final load incremental step

Fig.3 shows the plastically deformed region at the final load incremental step. It can be seen from Fig.3 that the plastically deformed region has a little bias towards the right edge of the quadrant of the plate.

The variation of the stress intensity factor K_{I} with loading and its comparison with the linear elastic solution of the finite element method (LFEM) are shown in Fig.4. It can be seen from Fig.4 that K_{I} obtained by the elasto-plastic solution is larger than that by the linear elastic solution of the finite element method, which are analyzed using FEM software-ANSYS, when loading reaches 0.2GPa, and their difference constantly increases with increasement of loading.

The variation of displacement normal to the crack direction u_y with loading and its comparison with results of FEM are shown in Fig.5. Both results have a good agreement.

Fig.6 shows the variation of the effective stress $\overline{\sigma}$ with distances r between front of the crack tip and the crack tip and its comparison with results of FEM. It can be seen from Fig.6 that the effective stress $\overline{\sigma}$ gradually decreases with increasement of the distances. Both results have a little difference

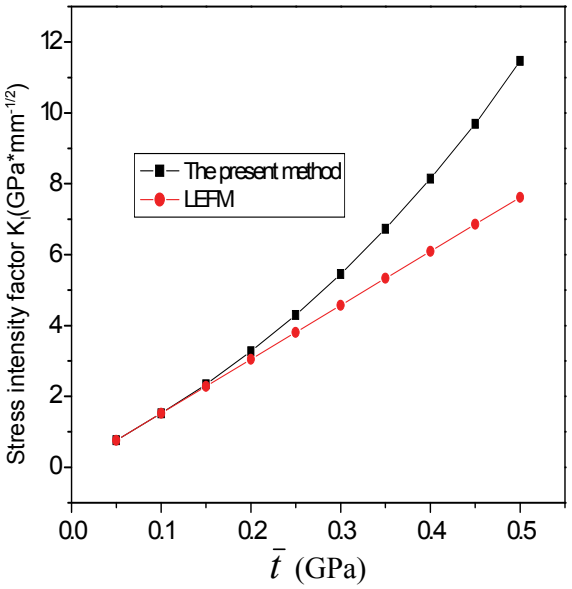

Figure 4: The variation of the stress intensity factor

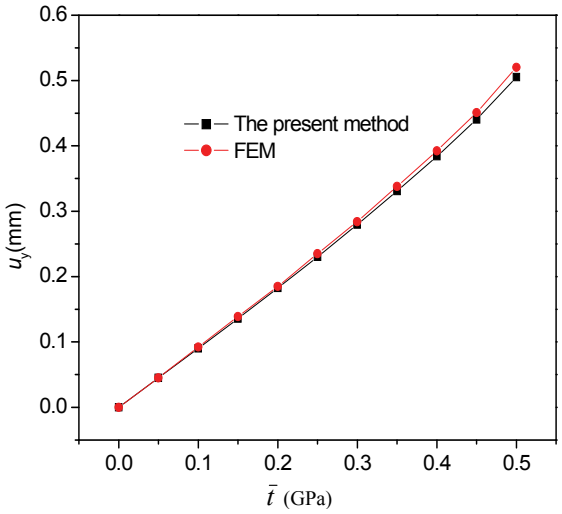

Figure 5: The variation of displacement normal to the crack direction u_y with loading

with the largest error being less than 7%.

Fig.7 also shows the variation of the effective stress $\overline{\sigma}$ at the crack tip with loading and its comparison with results of FEM. It can be seen from Fig.7 that results obtained by the present method are a little larger than that by FEM, but both results have the same variation trend.

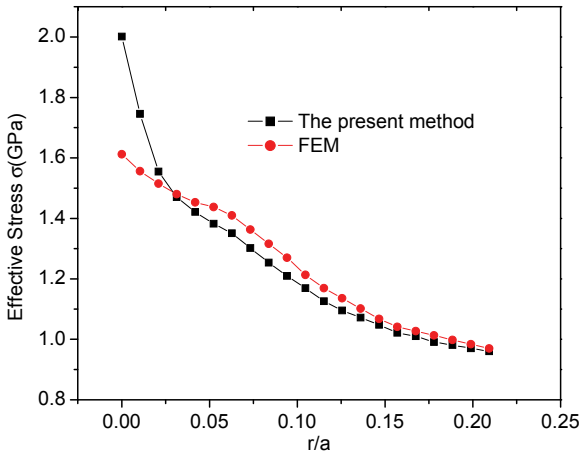

Figure 6: The effective stress $\overline{\sigma}(\theta = 0)$ in front of the crack tip and comparison with results of FEM.

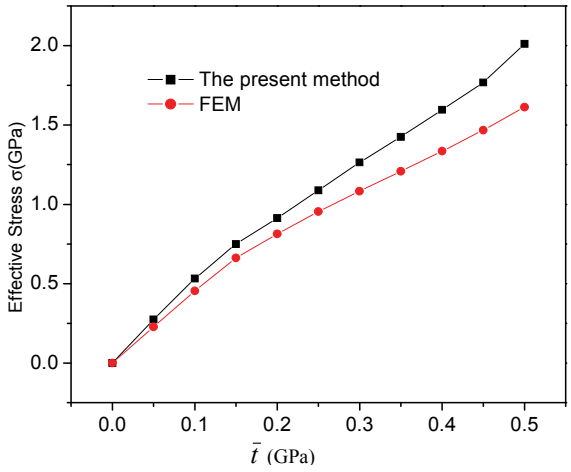

Figure 7: The variation of the effective stress $\overline{\sigma}$ at the crack tip with loading

5.2 *Example 2: a three-point bending sample*

Consider a three-point bending sample with length $L = 5$m, height $H = 1$m, thickness $t = 0.1$m, as shown in Fig.8. An edge-crack with length $a = 0.25$m lies at the middle of the sample, and two simply-supports are imposed at a distance $L_s/2 = 2.25$m from the crack. A concentrated force $P = 2$kN is applied at the middle of the sample. Here assume elastic modulus $E = 200$GPa, Poisson's ratio $\nu = 0.3$, the tangent elastic modulus $E^t = 100$GPa, the initial yield

stress $\sigma_{s0} = 20$MPa. Due to symmetry of geometry, load and supported conditions, one half of the sample is analyzed and is assumed to be the plane stress problem. In computation, a meshless discretization consisting of 887 nodes is used and symmetric displacement boundary conditions are imposed, as shown in Fig.9. The load increment is taken as $\Delta P = 0.05 \times P$, i.e. 20 load incremental steps are divided.

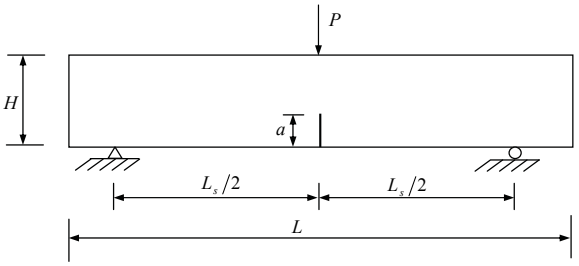

Figure 8: A three-point bending sample

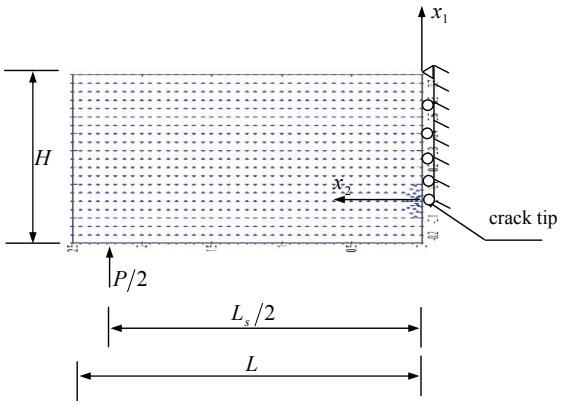

Figure 9: A meshless discretization(887nodes) and boundary conditions

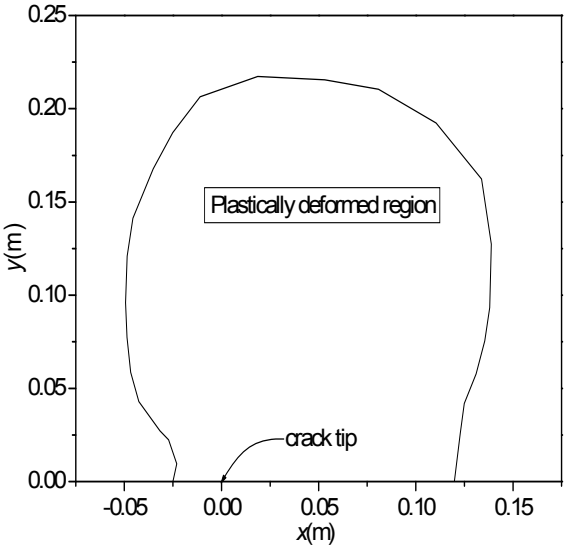

Figure 10: The plastically deformed region at the final load incremental step

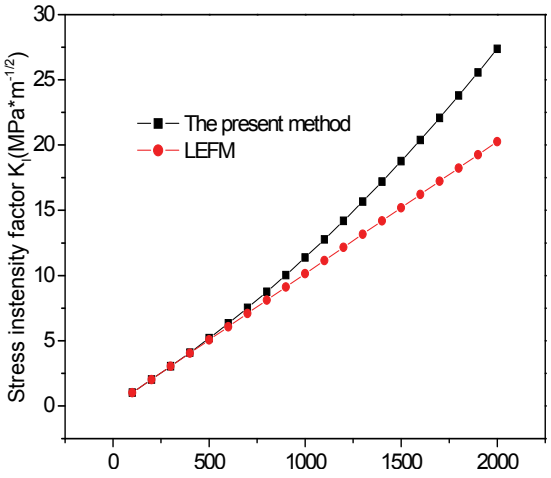

Figure 11: The variation of the stress intensity factor K_{I} with loading

Fig.10 displays the plastically deformed region at the final load incremental step. The variation of the stress intensity factor K_{I} with loading and its comparison with results of FEM are plotted in Fig.11. It can be seen from Fig.11 that when loading reaches 700N, K_{I} obtained by the elasto-plastic solution is larger than that by the linear elastic solution, and their difference constantly increases with increasement of loading. Fig.12 displays the variation of the opening displacements δ at the crack mouth with loading and its comparison with results of FEM. Both results have a good agreement.

6 Conclusions

The meshless local Petrov-Galerkin (MLPG) method that uses the Heaviside function as a

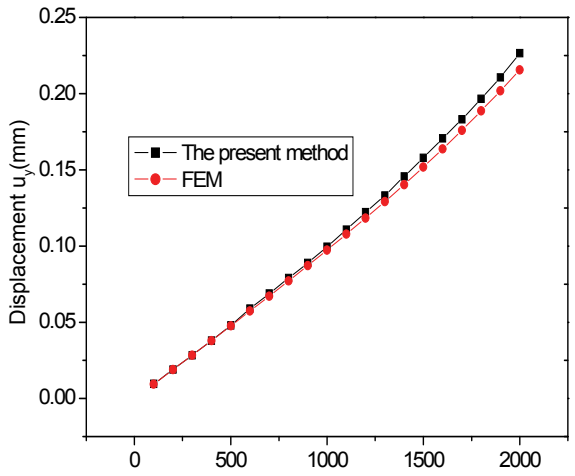

Figure 12: The variation of the opening displacements δ at the crack mouth with loading

test function is presented and used to analyze the elasto-plastic fracture problem in this study. The present results have a good agreement compared with the results obtained by using FEM software—ANYSY. However, in the present method, the computational time is greatly reduced in forming the tangent stiffness matrix if body force is ignored because there is no domain integral, and the pre- and post-processing time are also greatly reduced because no element connectivity and no remeshing are required. Two numerical examples indicate the proposed method possesses no numerical difficulties in the analysis of the elasto-plastic fracture problem.

Acknowledgement: This work was supported by National 973 Scientific and Technological Innovation Project(2004CB719402),Natural Science Foundation of China (No. 10672055), The Key Project of NSFC (No. 60635020) and The Natural Science Foundation for Outstanding Youth (No. 50625519).

References

Atluri S.N.; Zhu T. (1998): A new meshless local Petrov-Galerkin (MLPG) approach in computational mechanics. *Comput Mech*, 22, 117–127.

Lin H,; Atluri S.N. (2000): The meshless local Petrov-Galerkin (MLPG) method for solving convection-diffusion problem. *CMES: Computer Modeling in Engineering & Sciences*, 1, 45–60.

Ching H.K.; Batra R.C. (2001): Determination of crack tip fields in linear elastostatics by the meshless local Petrov-Galerkin (MLPG) method. *CMES: Computer Modeling in Engineering & Sciences* , 2, 273–290.

Sladek J.; Sladek V.; Krivacek J.; et al. (2005): Meshless local Petrov-Galerkin method for stress and crack analysis in 3-D axisymmetric FGM bodies. *CMES: Computer Modeling in Engineering & Sciences*, 8, 259–270.

Gao L.; Liu K.; Liu Y. (2006): Applications of MLPG method in dynamic fracture problems. *CMES: Computer Modeling in Engineering & Sciences*, 12, 181–195.

Sladek J.; Sladek V.; Zhang C.; et al. (2007a): Fracture analyses in continuously nonhomogeneous piezoelectric solids by the MLPG. *CMES: Computer Modeling in Engineering & Sciences*, 19, 247–262.

Long S.Y.; Atluri S.N. (2002): A meshless local Petrov-Galerkin (MLPG) formulation for solving the bending problem of a thin plate. *CMES: Computer Modeling in Engineering & Sciences*, 3, 53–63.

Gu Y.T.; Liu G.R. (2001): A meshless local Petrov-Galerkin (MLPG) formulation for static and free vibration analysis of thin plates. *CMES: Computer Modeling in Engineering & Sciences*, 2, 463–476.

Sladek J.; Sladek V.; Wen P.H.; et al. (2006a): Meshless local Petrov-Galerkin (MLPG) method for shear deformable shells analysis. *CMES: Computer Modeling in Engineering & Sciences*, 13, 103–117.

Jarak T.; Soric J.; Hoster J. (2007): Analysis of shell deformation responses by the meshless local Petrov-Galerkin approach (MLPG). *CMES: Computer Modeling in Engineering & Sciences*, 18, 235–246.

Sladek J.; Sladek V.; Atluri S.N. (2004): Meshless local Petrov-Galerkin method for heat conduction problem in an anisotropic medium. *CMES: Computer Modeling in Engineering &*

Sciences, 6, 309–318.

Wu X.H.; Shen S.P.; Tao W.Q. (2007): Meshless local Petrov-Galerkin collocation method for two-dimensional heat conduction problems. *CMES: Computer Modeling in Engineering & Sciences*, 22, 65–76.

Ching H.K.; Chen J.K. (2006): Thermomechanical analysis of functionally graded composites under laser heating by the MLPG method. *CMES: Computer Modeling in Engineering & Sciences,* 13, 199–217.

Sladek J.; Sladek V.; Zhang C.; et al. (2006b): Meshless local Petrov-Galerkin method for linear coupled thermoelastic analysis. *CMES: Computer Modeling in Engineering & Sciences*, 16, 57–68.

Sladek J.; Sladek V.; Zhang C.; et al. (2007b): Application of the MLPG to thermo-piezoelectricity.*CMES: Computer Modeling in Engineering & Sciences*, 22, 217–233.

Johnson J.N.; Owen J.M. (2007): A meshless local petrov-galerkin method for magnetic diffusion in non-magnetic conductors. *CMES: Computer Modeling in Engineering & Sciences*, 22, 165–188.

Ma Q.W. (2005): MLPG method based on Rankine source solution for simulating nonlinear water waves. *CMES: Computer Modeling in Engineering & Sciences*, 9, 193–209.

Ma Q.W. (2007): Numerical generation of freak waves using MLPG_R and QALE-FEM Methods. *CMES: Computer Modeling in Engineering & Sciences*, 18, 223–234.

Han Z.D.; Liu H.T.; Rajendran A.M.; et al. (2006): The applications of meshless local Petrov-Galerkin (MLPG) approaches in high-speed impact, penetration and perforation problems. *CMES: Computer Modeling in Engineering & Sciences*, 14, 119–128.

Liu H.T.; Han Z.D.; Rajendran A.M.; et al. (2006): Computational modeling of impact response with the RG damage model and the Meshless Local Petrov-Galerkin (MLPG)approaches. *CMC: Computers,Materials &Continua,* 4, 43–53.

Han Z.D.; Rajendran A.M.; Atluri S.N. (2005): Meshless Local Petrov-Galerkin (MLPG) approaches for solving nonlinear problems with large deformations and rotations. *CMES: Computer Modeling in Engineering & Sciences*, 10, 1–12.

Han Z.D.; Atluri S.N.(2004): A Meshless Local Petrov-Galerkin (MLPG) approach for3-dimensionalelasto-dynamics. *CMC: Computers,Materials &Continua*, 1, 129–140.

Andreaus U.; Batra R.C.; Porfiri M. (2004): Vibrations of cracked Euler-Bernoulli beams using Meshless Local Petrov-Galerkin (MLPG) method. *CMES: Computer Modeling in Engineering & Sciences*, 9, 111–131.

Shen S.P.; Atluri S.N. (2004): Multiscale simulation based on the meshless local Petrov-Galerkin (MLPG) method. *CMES: Computer Modeling in Engineering & Sciences*, 5, 235–255.

Atluri S.N.; Shen S. (2002): The meshless local Petrov-Galerkin (MLPG) method: a simple & less-costly alternative to the finite element and boundary element methods. *CMES: Computer Modeling in Engineering & Sciences*, 3, 11–51.

Hu D.A.; Long S.Y.; et al. (2006): A modified meshless local Petrov-Galerkin method to elasticity problems in computer modeling and simulation. *Engineering Analysis with Boundary Elements*, 30, 399–404.

Long S.Y.; Liu K.Y.; et al. (2006): A new meshless method based on MLPG for elastic dynamic problem. *Engineering Analysis with Boundary Elements,* 30, 43–48.

Liu K.Y.; Long S.Y.; et al. (2006): A simple and less-costly meshless local Petrov-Galerkin (MLPG) method for the dynamic fracture problem. *Engineering Analysis with Boundary Elements*, 30, 72–76.

Lancaster P.; Salkauskas K. (1981): Surfaces generated by moving least squares methods. *Math Comput*, 37, 141–158.

Liu G.R.; Yan L. (2000): A modified meshless local Petrov-Galerkin method for solid mechanics[P]. In: Atluri S N, Brust F W, editors. Advances in Computational Engineering and Science. Palmdale, CA: Tech Science Press, 1374–

1379.

Crisfield M.A. (1991): *Non-linear Finite Element Analysis of Solids And Structures Vol.1*. Chichester, England: John Wiley & Sons Ltd.

Owen D.R.J.; Hinton E. (1980): *Finite Element in Plasticity: Theory And Practice*. Swansea, UK: Pineridge Press Limited.

Wang X.C.; Shao M. (1997): *Basic Principle of Finite Element Method and Numerical Methods*. Beijing, China: Tsinghua University Press.

Liu GR.; Gu Y.T. (2005): *An Introduction to meshless Methods and Their Programming*. Dordrecht, The Netherlands: Springer.